

Modelling growth of chili pepper (*Capsicum annuum L.*) with the WOFOST model

Ruoling Tang ^{a,b,*}, Iwan Supit ^b, Ronald Hutjes ^b, Fen Zhang ^{a,d}, Xiaozhong Wang ^{a,d}, Xuanjing Chen ^{a,c,*}, Fusuo Zhang ^{a,c}, Xinping Chen ^a

^a Interdisciplinary Research Center for Agriculture Green Development in Yangtze River Basin, College of Resources and Environment, Southwest University, Chongqing 400716, China

^b Water Systems and Global Change Group, Wageningen University & Research, Droevedaalsesteeg 4, 6708, PB, Wageningen, the Netherlands

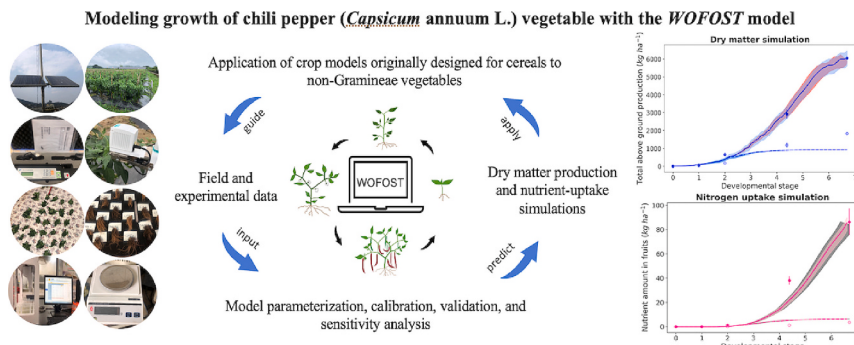
^c College of Resources and Environmental Sciences, National Academy of Agriculture Green Development, Key Laboratory of Plant-Soil Interactions, Ministry of Education, China Agricultural University, 2 Yuanmingyuan West Road, Beijing 100193, China

^d Academy of Agricultural Science, Southwest University, Chongqing, China

HIGHLIGHTS

- WOFOST was adapted for Chili simulation for the first time.
- A continuous 3-year field trial dataset was used for model calibration and validation.
- WOFOST-Chili is able to reproduce both potential and nutrient-limited growth.
- Systematic sensitivity analysis increased the robustness of model simulation.

GRAPHICAL ABSTRACT



ARTICLE INFO

Editor Name: Dr. Guillaume Martin

Keywords:

Chili pepper
WOFOST
Fertilizer response
Nutrient uptake
Dry matter production
Sensitivity analysis

ABSTRACT

CONTEXT: Chili pepper (*Capsicum annuum L.*) is one of the most economically and agriculturally important, and relatively nutrient-dense, vegetables that has, to date, received little attention in model studies relevant to dry matter production and nutrient-uptake predictions. There is an urgent need for models to analyse the potential impacts of climate change, as well as responsive adaptation options, while simultaneously optimising productivity against fertilizer use to reduce nutrient pollution.

OBJECTIVE: We adapted the WOrld FOod STudies (WOFOST) crop growth simulation model for chili pepper (WOFOST-Chili) to quantify dry matter production as a function of fertilizer management, climate, and soil conditions.

METHODS: We used 2021 field trial data under optimal growing conditions in southwestern China to parameterise and calibrate WOFOST-Chili. The model was tested under no-fertilizer conditions and further validated with data from 2019 and 2020. In addition, a sensitivity analysis over the three consecutive years was performed.

* Corresponding authors.

E-mail addresses: ruoling.tang@wur.nl (R. Tang), cjx0214@email.swu.edu.cn (X. Chen).

RESULTS AND CONCLUSIONS: Overall, the developed *WOFOST-Chili* model shows good simulations of chili growth dynamics in response to nitrogen (N) fertilization, both on biomass assimilation ($rRMSE = 0.07$ for total aboveground production; $rRMSE = 0.06$ for fruit dry weight) and nutrient uptake ($rRMSE = 0.46$ for leaf N amount; $rRMSE = 0.29$ for fruit N amount). Additionally, model robustness is increased by the sensitivity analysis of crop initialisation (e.g., biomass and leaf area index at transplanting) and climate-dependent parameters (e.g., temperature sums determining development rate and light use efficiency determining productivity), with the resulting wider simulation range covering more observations. This good performance is only limited by a weaker leaf area index (LAI) simulation ($rRMSE = 0.76$), which is partially attributed measurement limitations (e.g., equipment, weather conditions and labour/time constraints). Model validation confirms good performance under potential conditions, which is slightly reduced under nutrient-limited conditions.

SIGNIFICANCE: These findings improve our understanding of yield-nutrient interactions of chili pepper. They provide insight on expanding the application of crop models originally designed for cereals to non-Gramineae vegetables, while calling for future improvement of model accuracy under different fertilizer application strategies.

1. Introduction

Chili pepper is one of the world's most economically and agriculturally important vegetables in terms of cultivation area, production, commercial value, and consumption (FAOSTAT, 2020). The main production areas are located in warm and humid regions with temperatures around 18 to 30 °C (Khairov et al., 2019), for example the Yangtze River basin in China, Chihuahua in Mexico (Producepay, 2021), or the Black Sea region in Turkey. Recommended by the World Health Organization's Global Strategy on Diet, Physical Activity and Health, adults should intake at least 400 g d⁻¹ of fruit and vegetable per capita (Cammarano et al., 2022). More attention has been given to chili production due to its positive health benefits, being rich in vitamins E and C, provitamin A, dietary fibre, capsaicin, and other bioactive compounds (Baenas et al., 2019). Moreover, chili pepper may help reduce the mortality of cardiovascular diseases and cancer (Kaur et al., 2022).

In open-field production, due to their shallow rooting system and short lifespan, nutrients released from soil fertility generally do not match the needs of vegetables (Liu et al., 2012; Tei et al., 2020). On the one hand, yield loss may occur without applying extra fertilizer. If the field is over-fertilized, however, inhibitory effects on plant growth (e.g., crop yield reduction) combined with serious nutrient pollution may occur (Lu and Tian, 2017). To address food (especially nutrition) and environmental security, fertilizer management should be optimized and adapted to local conditions. Most of the existing research on the impact of fertilizer management on chili yield has been done at site-specific field level experiments (Stan et al., 2021; Wang et al., 2018). Each study utilized a distinct set of farming practices that were specific to the local area, involving fertilizer application dates and rates, fertilizer placement methods (broadcasting, banding, or side-dressing), the composition of fertilizer products, and other field management practices. For this reason, site-specific experiments make it challenging to replicate the productivity achieved with optimal management in other areas. Thus, there is a growing need for an upscaled study of quantitative relationships among plants, fertilizer management, and climatic conditions. Such a study could enhance potential yield prediction, policy formulation on fertilizer needs, and regional planting area distribution for the most suitable vegetable growing locations.

Crop models are regarded as useful tools for studying the interactions among crop physiology, agro-management, and the environment to support better decision-making in real production systems. Most of the crop modelling studies that investigated fertilizer influence have concentrated on wheat, maize, rice, and potato, while fruits and vegetables have received less attention (Kadigi et al., 2020; Liu et al., 2021; Tahir et al., 2021; Timsina et al., 2021). Research on the development of growth models for pepper crops remains scarce, not to mention yield response to different fertilizer strategies (Saqib and Anjum, 2021). Some earlier studies developed mechanistic sweet pepper models to examine physiological processes such as photosynthesis, dry matter partitioning, and nutrient uptake (Diao et al., 2009; Marcelis et al., 2004). For

example, based on the INTKAM model (Gijzen, 1994), Marcelis et al. (2004) created a mechanistic model for sweet pepper by combining a photosynthesis-driven cucumber model (Marcelis, 1994) for the dry matter production and partitioning with a nutrient uptake routine from a tomato model (Marcelis et al., 2003). Those plant-nutrient relations were obtained under well-controlled greenhouse conditions of soilless cultivation, however, and cannot be directly applied to open-field production prediction. In addition to mechanistic models, process-based pepper models were also reported in previous studies. One process-based "VegSyst" model was found to simulate both dry matter production and nitrogen (N) uptake of sweet pepper, but only under non-limiting water and N conditions and within Mediterranean-type greenhouses (Giménez et al., 2013). The latest pepper version, VegSyst V2, assumes a single growth phase with a uniform set of crop parameters (including a singular RUE value) to simulate the entire growing stage. The "one-single phase" modelling approach poses no issues when simulating peppers grown in greenhouses in Southeast Spain, as they are typically harvested before plants reach full maturity because of market reasons (Gallardo et al., 2016). This modelling approach cannot directly be used to simulate open-field peppers, however, which follow more indeterminate growth patterns and multiple fruit maturities. Another process-oriented pepper model *CROPGRO-Bellpepper* (CROP GROWth) is found to simulate yield response to 5 incremental N levels from 0 to 100 kg ha⁻¹ through fertigation in open-fields. However, no nutrient uptake simulation results were shown in this particular study (Reddy and Tiwari, 2018). To the best of our knowledge, while the *CROPGRO* model has been successfully employed to simulate crop N demand, soil N balance, and crop N uptake in other crops, its effectiveness in modelling nutrient uptake in pepper crops remains unexplored (Boote et al., 2008; Boote et al., 2018; Mendez, 2000). Growth and nutrient uptake simulations of open-field bell pepper was also found in EU-Rotate N (Doltra and Muñoz, 2010), a largely process-based model. However, a maximum achievable yield needs to be provided based on the user's experience before running the simulations (Øvsthus et al., 2021). In this case, dynamic crop growth prediction will be limited once the targeted yield data is unavailable. WOrld FOod STudies (*WOFOST*) is well known for simulating open-field crop production. In addition, compared with other crop models (e.g., APSIM, EPIC, CROPSYST, and STICS), *WOFOST* showed a similar performance of dry matter production response with the least complex level of N dynamics (Di Paola et al., 2016; Salo et al., 2016). However, we still lack an appropriate model approach that tracks both dynamic dry matter production and crop nutrient uptake under various fertilizer strategies, climate, and soil conditions for chili pepper in open-field production (including the *WOFOST* model).

Our research aims to explore the possibility of expanding the application of the crop model *WOFOST*, originally designed for cereals, to vegetables, (particularly chilis). To this end, we (i) parameterised, calibrated, and validated the developed *WOFOST-Chili* model using three consecutive years of observed field trial data, (ii) evaluated model performance under both potential and nutrient-deficient conditions, and

(iii) performed a sensitivity analysis to assess the robustness of model simulations.

2. Materials and methods

2.1. WOFOST-chili model overview

WOFOST is a process-based crop model run at daily time steps that simulates several physiological processes, such as phenological development, photosynthesis-driven assimilation, respiration, transpiration, leaf, stem, grain and root dynamics, nutrient uptake, and partitioning among plant components. Two major issues were addressed in the adaptation of *WOFOST-Chili*: (i) redefinition of key developmental stages (transplanting, anthesis, early-fruitlet, mid-fruitlet, peak-fruitlet/harvest; Fig. 1) and (ii) recalculation of key parameters using observed data (Table 1, Table 2). In the standard Biologische Bundesanstalt, Bundesortenamt and Chemical industry (BBCH) scale, 9 stages are used to completely describe the lifecycle of chili pepper, starting from seed germination to senescence (Meier, 1997). Normally, in actual production systems, the growing stages are not distinguished so precisely since fruit dry matter receives the most attention. Therefore, we redefined chili's development stage (DVS) based on several rounds of fruit maturity. In the developed *WOFOST-Chili* model, TSUM1 was redefined as the required temperature sum (TSUM) from transplanting to anthesis. TSUM2 was redefined as the required TSUM from anthesis to early-fruitlet stage. We kept the anthesis stage as DVS = 1, and the early-fruitlet stage as DVS = 2. The next two fruit maturity stages were at mid-fruitlet stage and peak-fruitlet stage/harvest, whereas the matching DVS was calculated as 2 plus the accumulated TSUM from the early fruiting stage to the present stage, divided by TSUM2 (Fig. 1), as shown in Eq. 1.

$$DVS = 2 + \frac{TSUM - TSUM2}{TSUM2} \quad (1)$$

Where DVS is the developmental stage, TSUM is total temperature sum from transplanting to present stage. TSUM2 is the temperature sum from anthesis to early-fruitlet stage.

2.2. Field experiments

An open-field experiment was conducted in Hechuan, Chongqing, China (30.0° N; 106.1° E) from 2019 to 2021. The site has a subtropical monsoon humid climate. Weather inputs required to run the *WOFOST-Chili* were collected from an on-site weather station. A commercial chili pepper variety 'Xinxiang #8' was grown under rain-fed conditions on the Haplic Luvisol soil site with the recommended planting density of $3.4 \text{ plants m}^{-2}$. Six different N fertilizer treatments were designed: control treatment without applying any fertilizer (CK), optimal amount of synthetic fertilizer (OPT), excessive synthetic fertilizer following local farmers' regular practice (FNP), mixed organic and synthetic fertilizer (OIF), denitrification fertilizer products (DMPP), and slow control-release fertilizer products (SCR). All treatments were laid out in a Randomized Complete Block Design with 4 replicates. Plants were transplanted on 20 May, 12 May, 27 April and harvested on 10 August, 6 August and 25 July in 2021, 2020 and 2019, respectively. Fertilizers were applied during transplantation, followed in three split applications of anthesis, early-fruitlet, and mid-fruitlet (Fig. 1). The average daily precipitation within the chili growing season was 7 mm day^{-1} and 6 mm day^{-1} in 2019 and 2020, respectively, and rather evenly distributed. In 2021 it was 4 mm day^{-1} , but more concentrated around 40–60 days after transplanting (ddt). We assumed no water limitation, even without regular irrigation (Annex 1, Fig. S2). Best agronomic practices were applied to minimize risks of yield loss by insects, pathogens, and weeds. The detailed fertilizer components and amounts, crop management, plot design, and site weather information are presented in Annex 1 (Table S1; Fig. S1; Fig. S2).

Non-destructive physiological assessments, including maximum leaf

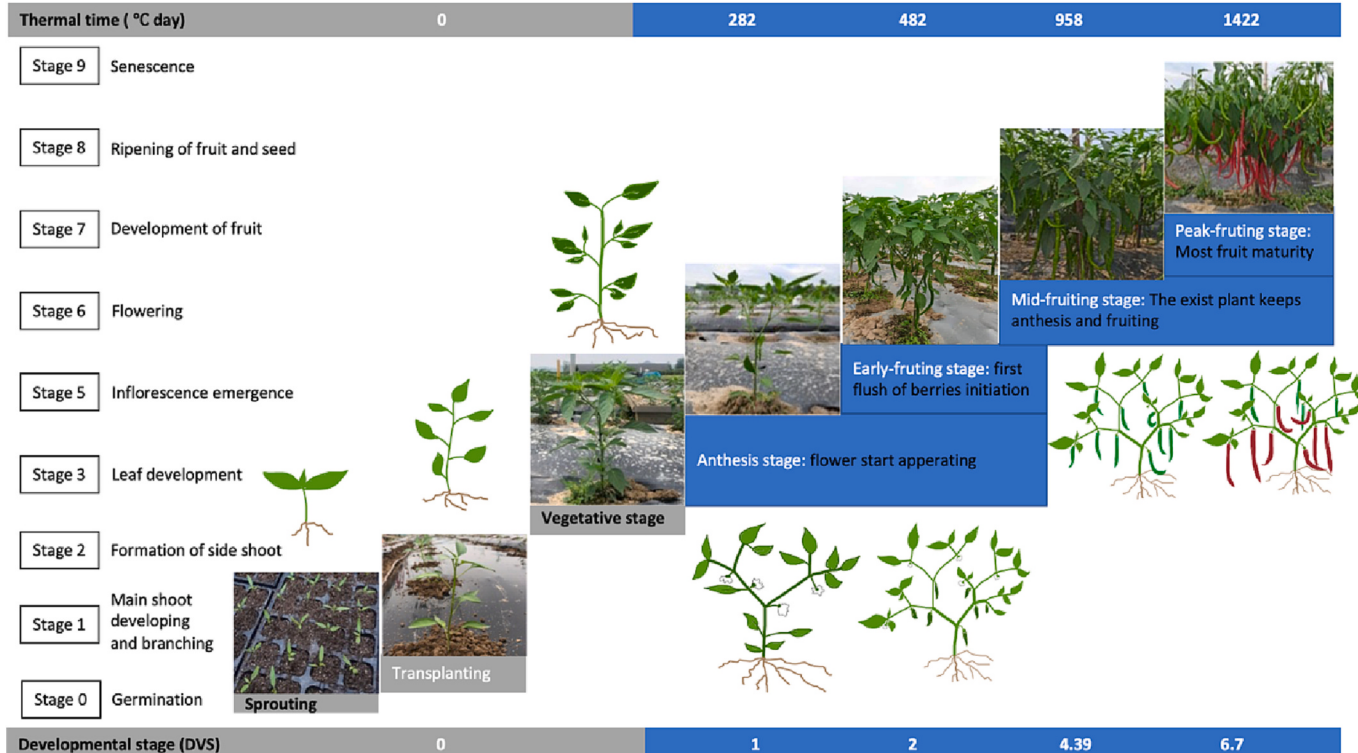


Fig. 1. Illustrative phenological growth pattern of chili pepper. The key developmental stages of *WOFOST-Chili* are displayed on the horizontal axis at the bottom, with the corresponding temperature sums at the top. On the vertical axis, the growth of chili pepper is described, using the Biologische Bundesanstalt, Bundesortenamt and Chemical industry scale.

Table 1

Scalar parameter values within WOFOST-Chili crop file that are parameterized with observed data (year 2021) and each is represented by a single numerical value.

Abbreviations	Description of scalar parameters	Categories	Calibrated Value
TSUMEM	Temperature sum from sowing to transplanting [cel d]	Emergence	644
TSUM1	Temperature sum from transplanting to anthesis [cel d]	phenology	282
TSUM2	Temperature sum from anthesis to fruiting [cel d]		200
TDWI	Initial total crop dry weight [kg ha ⁻¹]		16.17
LAIEM	Leaf area index at emergence [ha ha ⁻¹]	Initial	0.0106
RGRLAI	Maximum relative increase in LAI [ha ha ⁻¹ d ⁻¹]		0.039
NPK_TRA	N-P-K translocations from roots as a fraction of resp. Total N-P-K amounts translocated from leaves and stems		0.30
NMAXRT_FR	Maximum N concentration in roots as fraction of maximum N concentration in leaves		0.22
NMAXST_FR	Maximum N concentration in stems as fraction of maximum N concentration in leaves		0.26
PMAXRT_FR	Maximum P concentration in roots as fraction of maximum P concentration in leaves		0.605
PMAXST_FR	Maximum P concentration in stems as fraction of maximum P concentration in leaves	Nutrient use	0.737
KMAXRT_FR	Maximum K concentration in roots as fraction of maximum K concentration in leaves		0.719
KMAXST_FR	Maximum K concentration in stems as fraction of maximum K concentration in leaves		0.955
NMAXSO	Maximum N concentration (= 1.6*min. N conc.) In storage organs [kg N kg ⁻¹ dry biomass]		0.0365
PMAXSO	Maximum P concentration (= 1.6*min. P conc.) In storage organs [kg P kg ⁻¹ dry biomass]		0.0060
KMAXSO	Maximum K concentration (= 1.6*min. K conc.) In storage organs [kg K kg ⁻¹ dry biomass]		0.0326

CO₂ assimilation rate at light saturation point (Amax) and light use efficiency (EFF), were executed on plants at transplanting, anthesis, early-fruitlet, mid-fruitlet, and peak-fruitlet/harvest of year 2021. A series of periodic photosynthetic light responsive curve measurements were conducted with a Licor-6800 (LICOR, Lincoln, Nebraska, USA) on the uppermost fully expanded leaf of 3 representative plants within one selected plot per treatment. Fourteen desired levels of light intensity,

1800, 1500, 1300, 1100, 900, 700, 500, 300, 200, 150, 100, 70, 30, and 0 μmol m⁻² s⁻¹, were set with a minimum wait time of 120s, and a maximum wait time of 300s to reach a steady state before logging. These measurements were then used to fit a light response curve ([Prioul and Chartier, 1977](#)) to derive the model parameters Amax and EFF (See [Table 2](#) and S2A).

Destructive measurements for dry weight and N, phosphorus (P), and potassium (K) concentration of roots, stems, leaves, and fruits were conducted 5 times (from transplanting to harvest) during the 2021 season and 3 times (from early-fruitlet to harvest) during the 2019 and 2020 seasons. At each sampling we harvested all formed fruits with a length of at least 2 cm. Within each plot per treatment, 4 plants were mixed sampled and oven dried at 100 °C for the first hour and at 75 °C thereafter until reaching constant mass. After weighing, samples were finely ground and approximately 0.500 g per sample was digested with 5 ml of HNO₃ and 3 ml of H₂O₂ in a microwave-accelerated reaction system (CEM, Matthews, NC, USA) for NPK concentration analyses. Total N content was determined using the micro-Kjedahl method ([Bremner, 1996](#)). Total P and K concentrations were determined using an inductively coupled plasma optical emission spectrometer (ICP-OES) (OPTIMA 3300 DV, PerkinElmer, USA). The leaf area measurements were conducted 5 times (from transplanting to harvest) in 2021 using the portable Leaf Area Meter (YMJ-A, TOP-Cloud-agri, Hangzhou, CHN). Three repetitions per treatment were conducted. For the first 4 measurements, all leaves within one plant were picked, scanned and the leaf area was summed up. Due to the explosive increase in leaf numbers, however, leaf area per plant at harvest was derived by leaf area-leaf fresh weight ratios for three sub-sample measurements (each with a fresh weight of 5 ± 0.5 g).

The experimental data used to parameterise/calibrate and test the model in this study were from two fertilizer treatments: CK and DMPP. Treatment DMPP was selected as it showed the highest productivity and can effectively reduce the nitrogen leaching and N₂O emission by inhibiting the oxidation of ammonia, especially in rainy areas ([Zerulla et al., 2001](#)). The other fertilizer treatments did not significantly differ from DMPP in terms of fruit dry matter over three years, so all can be considered non-limited in terms of nutrients.

2.3. Model parameterisation, calibration and validation

WOFOST distinguishes two types of parameters in the crop file: (1) scalar parameters, which do not change with developmental stage (DVS) or environmental conditions, and (2) tabular parameters, that use pairs of values as a function of changing status ([de Wit et al., 2020](#)). As for the crop file, we obtained parameter values associated with phenology, green area, CO₂ assimilation, partitioning, and nutrient use from field observations, while the few remaining parameters were estimated from literature where possible ([Table 1](#); [Table 2](#); Annex 2, Table S2A and B). We used the data measured during the 2021 season for calibration of the model. The model output was compared with the observations in terms of the total aboveground production (TAGP), total dry weight of leaves

Table 2

Tabular parameter values within the parametrized WOFOST-Chili crop file that are parameterized with observed data (year 2021), and each is represented with a set of values in function of developmental stages (DVS).

Abbreviations	Description of tubular parameters	Categories	Calibrated Value (as a function of DVS)				
			DVS 0.0	DVS 1.0	DVS 2.0	DVS 4.39	DVS 6.7
SLATB	Specific leaf area [–; ha kg ⁻¹]						
AMAXTB	Max. Leaf co2 assimilation rate [–; kg ha ⁻¹ h ⁻¹]	Green area assimilation	0.0029	0.0018	0.0029	0.0027	0.0023
FRTB	Fraction of total dry matter to roots [–; kg kg ⁻¹]		34.84	37.13	55.73	49.64	30.49
FLTB	Fraction of above-gr. Dm to leaves [–; kg kg ⁻¹]		0.180	0.012	0.038	0.048	0.048
FSTB	Fraction of above-gr. Dm to stems [–; kg kg ⁻¹]	partitioning	0.500	0.630	0.500	0.086	0.143
FOTB	Fraction of above-gr. Dm to storage organ [–; kg kg ⁻¹]		0.500	0.370	0.217	0.195	0.178
NMAXLV_TB	Maximum N concentration in leaves [kg N kg ⁻¹ dry biomass]		0.000	0.000	0.283	0.719	0.679
PMAXLV_TB	Maximum P concentration in leaves [kg P kg ⁻¹ dry biomass]	nutrient use	0.0200	0.0150	0.0137	0.0133	0.0127
KMAXLV_TB	Maximum K concentration in leaves [kg K kg ⁻¹ dry biomass]		0.0023	0.0032	0.0051	0.0032	0.0020

(TWLV), total dry weight of storage organs (TWSO), total dry weight of stems (TWST); nitrogen/phosphorous/potassium amount within leaves (N/P/KamountLV), stems (N/P/KamountST), fruits (or storage organ: N/P/KamountSO), and roots (N/P/KamountRT); and leaf area index (LAI) at each sampling (Annex 4, Table S6). To minimize the differences between simulations and observations, several estimated parameters (e.g., specific leaf area, SLA, extinction coefficient for diffuse visible light, KDIF) were tuned to within the measured uncertainty range, or an otherwise reasonable range. In addition to the crop file, WOFOST requires the soil file and site file to compute the daily water and nutrient balance in the soil. These files provide essential information to the model about the location and soil characteristics of the field being modelled (Boogaard et al., 2014). To the best of our knowledge, main physical soil characteristics relevant to soil water retention, hydraulic conductivity, and soil workability, together with the background information of initial soil moisture status and initial soil nutrient availability, were parametrised in the soil file (Annex 2, Table S3) and the site file (Annex 2, Table S4) separately.

The calibrated WOFOST-Chili was thereafter tested using the on-site experiment of year 2019 and 2020. Recorded meteorological data for the year 2019 and 2020, together with the agro-management information (e.g., date of transplanting, harvest, and fertilization), were used to run the simulations in the farm. Unlike field experiment of year 2021, we conducted only 3 samplings per season in years 2019 and 2020, so comparisons between observations and simulations were limited to after fruiting (Table 3).

2.4. Model performance evaluation

We evaluated the performance of the WOFOST-Chili model mainly using the Coefficient of determination (R^2) and relative Root mean squared error (rRMSE). R^2 was classified as unsatisfactory ($R^2 \leq 0.6$), satisfactory ($0.6 < R^2 \leq 0.7$), good ($0.7 < R^2 \leq 0.8$) and very good ($R^2 > 0.8$) (Bosi et al., 2020). In addition, each R^2 was attached with a t-test P_t value to indicate the similarity between observed data and simulated data. The similarity was classified when $P_t < 0.05$. A value of zero for rRMSE means that the model predicts the observations with perfect accuracy. A value of ≤ 0.70 for rRMSE is considered acceptable for model performance (Moriasi et al., 2007). We also assisted WOFOST-Chili model evaluation with Nash-Sutcliffe model efficiency coefficient (NSE) and Willmott agreement index (d). Detailed information is provided in Annex 4 (Annex 4, Table S5).

2.5. Sensitivity analysis

We performed a systematic sensitivity analysis to identify high-impact parameters for model uncertainty. We first referred to experts' recommendations and literature to formulate a series of agrobiologically meaningful potential parameters and their reasonable range of changes, then conducted multiple sensitivity analyses. AMAXTB, SLATB, KDIFTB, EFFT, CVO, FLTB were given a $\pm 5\%$ fluctuation range as those parameters are easily influenced by temperature and radiation between different growing years. In the open-field production, plant initial status is more difficult to control, so we gave a larger fluctuation range ($\pm 25\%$) to initial biomass (IB), which was defined as a combination of parameter initial total crop dry weight (TDWI) and leaf area index at transplanting (LAIEM). Considering the recording variance of plant development stage, we varied ± 1 day to calculate temperature sum from transplanting to anthesis (TSUM1).

3. Results

3.1. Field observations of dry weight and nutrient-uptake of plant components

The DMPP treatment represented potential growth as it showed the highest fruit dry matter (3456 kg ha^{-1}) among all 6 treatments in 2021, although not significantly higher than the second most productive SCR treatment (3049 kg ha^{-1}) (Annex 3, Table S3). The fruit dry matter in DMPP was the highest in the 2021 harvest period and was significantly higher than that of CK in both 2019 and 2020 (Table 3; Annex 3, Table S3). Except for leaf dry weight and the leaf N amount in 2021, DMPP was significantly higher than CK on stem, leaf, and root dry weight and N amount (Table 3). As for P and K uptake which were only measured in 2021, DMPP was significantly higher than CK in terms of fruit P and K amount and leaf K amount, while the leaf P amount was not significantly different from CK (Annex 3, Table S3). A potential reason for the insignificant difference in leaf dry weight between DMPP and CK in the 2021 harvest period may be related to the discovery of an unexpectedly large number of fallen leaves which we did not account for in the leaf dry weight measurement (Annex 3, Table S4). This may also be the cause for the insignificantly higher amount of leaf N and P found in DMPP.

Table 3

Observed mean of dry matter (DM) and assimilated Nitrogen amount in leaves, stems, fruits, and roots for each of the years 2019 to 2021.

	2019		2020		2021	
	(kg ha ⁻¹)	CK	DMPP	CK	DMPP	CK
Stem DM	359 ± 115	1036 ± 68**	510 ± 239	1177 ± 189*	620 ± 194	1282 ± 417**
Leaf DM	158 ± 44	923 ± 88**	372 ± 106	1451 ± 290**	432 ± 16	1322 ± 103
Fruit DM	925 ± 207	3713 ± 208**	1074 ± 72	3831 ± 197**	965 ± 132	3456 ± 231*
Root DM	111 ± 12	244 ± 46**	129 ± 23	247 ± 38*	145 ± 59	202 ± 8**
(g N kg ⁻¹ DM)						
Stem N%	3.0 ± 0.6	16.0 ± 0.7**	4.1 ± 1.1	14.9 ± 1.4**	5.9 ± 0.5	13.2 ± 1.3*
Leaf N	5.1 ± 0.8	41.8 ± 2.2**	12.2 ± 1.9	64.9 ± 4.1**	15.3 ± 1.4	68.0 ± 2.6
Fruit N	12.7 ± 0.9	82.2 ± 3.9**	21.9 ± 1.2	101.2 ± 6.7**	19.8 ± 2.6	101.1 ± 6.0**
Root N	1.2 ± 0.2	3.4 ± 0.3**	1.3 ± 0.2	3.0 ± 0.2**	1.7 ± 0.4	3.2 ± 0.1**

Statistical comparisons are made independently for each year. Significance tests were done by Independent Samples t-Test, * means $P < 0.05$, ** means $P < 0.01$. t-test results of Root DM, Leaf N, and Fruit N in 2019 did not pass the Levene's Test for Equality of Variances, so we used Welch's ANOVA significance test instead. Calculated values were based on observed means of sampled DM at the end of the growing season, e.g., 4 repetitions in each year.

Green backgrounds indicate potential growth while grey backgrounds indicate nutrient-limited growth.

3.2. Calibrated potential simulations of chili dry matter production and nutrient-uptake

Fig. 2 and **Table 4** show that the predicted values are in good agreement with observed data for the dry matter-related traits evaluated in this study. The high values of R^2 (0.78–1.00) and P_t (0.57–0.99) indicate a good fit and insignificant difference between observed and predicted values. The high accuracy is also supported by the rRMSE. The potential fruit dry weight (TWSO) and total above ground production (TAGP) are well simulated with a rRMSE of 0.06 and 0.07 respectively. The leaf dry weight (TWLV) showed a rRMSE of 0.23, while the simulated leaf area index (LAI) (rRMSE = 0.76) has the worst agreement with the observations (**Fig. 2**). Prediction of fruit dry weight (TWSO) is the most accurate among all biomass variables, with a bias (135 kg ha^{-1}) at final harvest smaller than the observed standard deviation ($\text{SD} \pm 231 \text{ kg ha}^{-1}$). The model also reproduces observed values of total aboveground production (TAGP) very well with only +1.1% overestimation (52 kg ha^{-1}) at harvest, although there is a tendency to under-predict at the early-fruiting stage. Prediction of leaf dry weight (TWLV) is less accurate than TWSO and TAGP, with a – 21% underestimation in the early-fruiting stage and a + 32% overestimation at the mid-fruiting stage.

This fluctuation results in a good agreement at final harvest, with a smaller bias (50 kg ha^{-1}) than the observed standard deviation ($\text{SD} \pm 51 \text{ kg ha}^{-1}$). The LAI is the least accurately predicted because the simulated curve peaks after the mid-fruiting stage and then gradually decreases. The simulated LAI is almost twice as high as the measurement at the mid-fruiting stage and had a + 28% overestimation at final harvest.

Fig. 3 and **Table 4** show that the NPK uptake predictions are accurate in relation to R^2 value (0.78–0.99) and P_t (0.60–0.97). In terms of rRMSE, however, model simulation of nutrient uptake is generally inferior to dry matter simulation, with N amount in fruits (rRMSE = 0.29) and leaves (rRMSE = 0.46), P amount in fruits (rRMSE = 0.39) and leaves (rRMSE = 0.43), and K amount in fruits (rRMSE = 0.46) and leaves (rRMSE = 0.30) (**Table 4**). The simulated NPK amount curves in leaves shows a rising trend due to nutrient uptake and then decreasing due to nutrient translocation. The earliest nutrient translocation from leaves to fruits occurs in leaf P amount before the mid-fruiting stage, followed by leaf K amount, and then leaf N amount around harvest. In contrast, the simulated NPK amount curves in fruits rise continuously (**Fig. 3**). Our model underestimates NPK amount in leaves at the early-fruiting stage (N: -20%; P: -4%; K: -6%), overestimates at the mid-fruiting stage (N: +33%; P: +37%; K: +33%), and underestimates

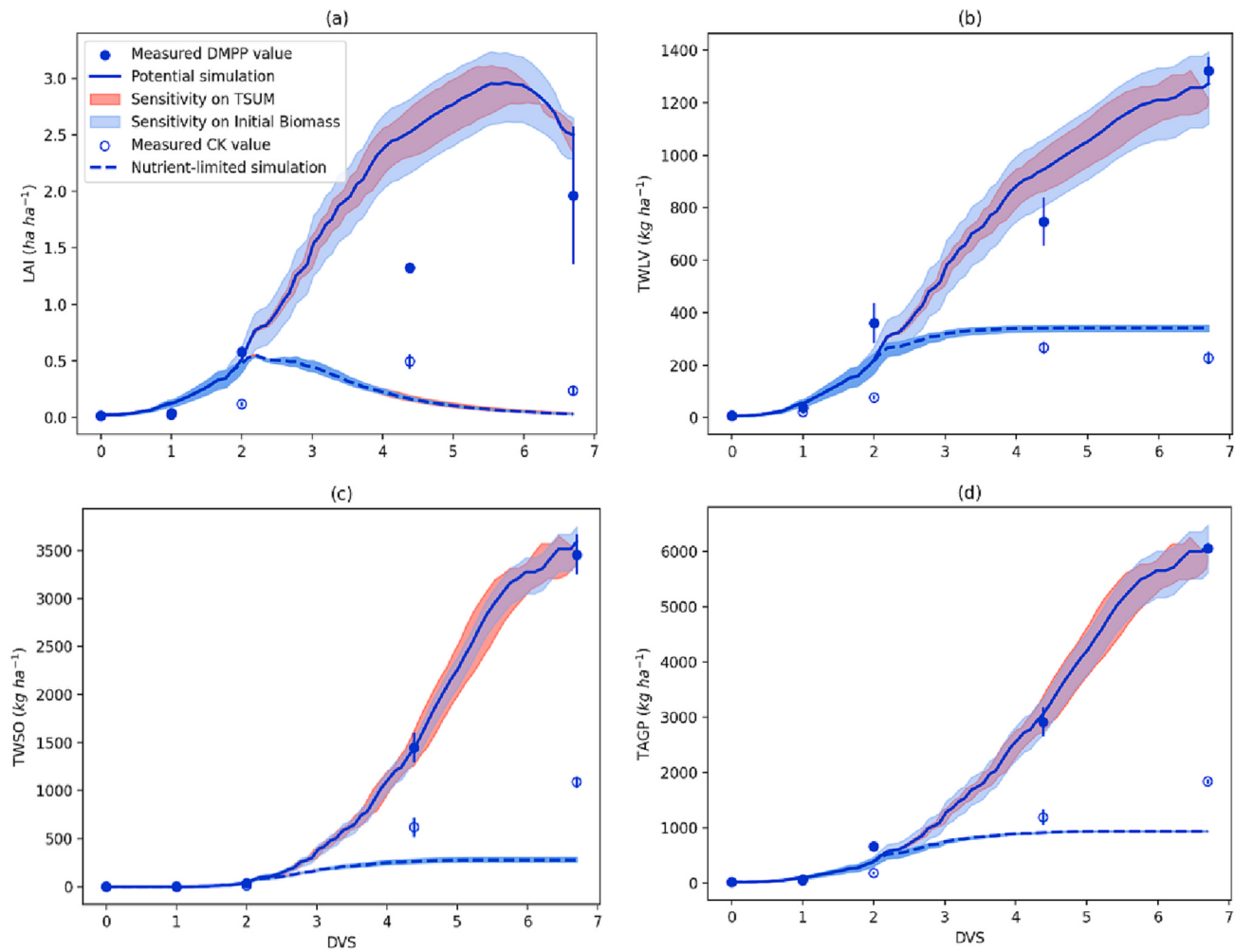


Fig. 2. Model-simulated and observed values of (a) leaf area index (LAI), (b) total leaf dry weight (TWLV), (c) total fruit dry weight (TWSO), and (d) total above ground production (TAGP) for model calibration (2021) and their sensitivity analyses, under both potential and nutrient-limited conditions. The x-axes represents developmental stages of chili, from transplanting (DVS = 0), anthesis (DVS = 1), early-fruiting stage (DVS = 2), mid-fruiting stage (DVS = 4.39), to peak-fruiting stage/harvest (DVS = 6.7). The continuous lines represent potential (PP) simulations and the dashed lines nutrient-limited (NL) simulations. Sensitivity on initial biomass at transplanting ($\pm 25\%$) is shown in the light-blue shaded areas while the red shaded areas represents variations within ± 1 day of temperature sum from transplanting to anthesis (TSUM1). Field data under denitrification fertilizer treatment (DMPP) are plotted in filled dots, while the no-fertilizer treatment (CK) is plotted in circles. Error bars indicate the standard deviation (SD) of observed values. (For interpretation of the references to colour in this figure legend, the reader is referred to the web version of this article.)

Table 4

WOFOST-Chili calibration (2021 dataset) and validation (2019 and 2020 datasets) for potential (PP, green background) simulation & nutrient-limited (NL, grey background) simulation. Red numbers indicate an unsatisfactory model performance.

PP simulation	R ² ^①			rRMSE ^②			NL simulation	R ² ^①			rRMSE ^②		
	C2021	V2020	V2019	C2021	V2020	V2019		C2021	V2020	V2019	C2021	V2020	V2019
TWLV	0.95	0.99	0.74	0.23	0.10	0.19	0.90	1.00	<u>0.00</u>	0.74	0.32	0.69	
TWSO	1.00	0.96	1.00	0.06	0.23	0.46	0.90	0.65	0.89	1.16	0.94	0.92	
TAGP	1.00	0.96	0.99	0.07	0.19	0.30	0.88	0.80	0.92	0.67	0.61	0.60	
NamountST	0.90	0.65	0.81	0.32	0.24	0.40	0.01	1.00	<u>0.79</u>	1.15	1.08	0.64	
NamountLV	0.82	0.96	0.62	0.46	0.16	0.17	0.04	0.89	0.94	1.26	0.92	0.53	
NamountSO	0.96	1.00	0.98	0.29	0.30	0.47	0.78	0.78	0.91	1.11	0.85	0.53	
NamountRT	0.96	0.84	0.72	0.39	0.44	0.40	0.05	<u>0.99</u>	<u>0.48</u>	1.26	0.87	0.85	
LAI				C2021			C2021			C2021		C2021	
PamountST												1.	
PamountLV												0.29	
PamountSO												0.65	
PamountRT												0.97	
KamountST												0.58	
KamountLV												0.50	
KamountSO												1.00	
KamountRT												0.54	

① Coefficient of determination: $R^2 = \frac{[\sum(Oi - Omean)(Pi - Pmean)]^2}{\sum(Oi - Omean)^2 \sum(Pi - Pmean)^2}$; was classified as unsatisfactory ($R^2 \leq 0.6$), satisfactory ($0.6 < R^2 \leq 0.7$), good ($0.7 < R^2 \leq 0.8$) and very good ($R^2 > 0.8$). If the R^2 value that did not pass the T. TEST, it was classified as $P_t \leq 0.05$ and underlined.

$$\text{② Relative Root mean squared error: } rRMSE = \sqrt{\left[\frac{1}{n} \sum_{i=1}^n (Pi - Oi)^2 \right] / Omean}$$

② Relative Root mean squared error: $rRMSE = \sqrt{\left[\frac{1}{n} \sum_{i=1}^n (Pi - Oi)^2 \right] / Omean}$; was classified as perfect accuracy ($rRMSE = 0$), acceptable ($rRMSE \leq 0.70$).

ST, LV, SO, RT are the abbreviations for stems, leaves, storage organs (fruits), and roots.

again at the final harvest (N: -29%; P: -26%; K: -20%). The simulated NPK amount in fruits is underestimated at the mid-fruiting stage (N: -44%; P: -24%; K: -32%). At final harvest, the fruit P amount is -19% underestimated and the fruit K amount is +17% overestimated, whereas fruit N amount is perfectly predicted (Fig. 3; Annex 4, Table S6). In general, apart from a weak model performance on K amount in roots ($rRMSE = 0.89$) (Annex 4, Fig. S3), WOFOST-Chili shows good performance on the model outcomes relevant to nutrient uptake simulations (Table 4).

Potential simulations are responsive to a $\pm 5\%$ adjustment of AMAXTB, EFFTBT, CVL, FLTB, KDIFTB, and SLATB (Annex 5, Fig. S5-S16), but are more sensitive when adjusting TSUM1 and IB (Figs. 2 & 3). Compared to fruit growth simulations, potential leaf growth simulations were found to be more sensitive to parameter changes. In 2021, when adjusting a $\pm 25\%$ IB, the potential simulated LAI, TWLV, and leaf NPK amount fluctuations at final harvest each respond by approximately -10% to +5%. The same adjustment resulted in less influence on potential simulations of TWSO and fruit NPK amounts, with about (-7%, +5%) at harvest. When adjusting the TSUM1 with the observed -12°C d (one day in advance) and $+15^\circ\text{C d}$ (one day postponed), potential leaf growth simulations are affected by approximately -6% to +7%. Similarly, it resulted in a less influence on fruit growth simulations, with (-3%, 1%) (Figs. 2 & 3). Overall, the sensitivity analysis extended the

ranges of potential simulation outcomes, implying that more observed values fall inside the sensitivity bands.

3.3. Comparison of calibrated nutrient-limited simulations with observations under CK treatment

The WOFOST-Chili model can simulate both potential (PP) and nutrient-limited (NL) conditions. We compare NL simulations with observations under the CK (no fertilizer) treatment in the field in Figs. 2 and 3 (dashed lines) and again in Table 4. For biomass-related traits, R^2 values (0.88– 0.90) indicate very good agreement between predicted and observed values, and the t -test indicates similarity ($P_t > 0.35$) between predicted and observed values for all biomass variables. Good model performance is only found in TAGP ($rRMSE = 0.67$) in terms of $rRMSE$ values, however, as the TWLV ($rRMSE = 0.74$), and TWSO ($rRMSE = 1.16$) are less acceptable (Table 4). In addition, our results indicate a relatively poor LAI simulation since both R^2 value (0.00) and $rRMSE$ value (1.38) are outside of the standard range of acceptable model performance ($R^2 > 0.60$; $rRMSE \leq 0.70$) (Table 4). In general, the NL configuration overestimates TWLV after anthesis stage, but underestimates TWSO after the early-fruiting stage, resulting in a + 131% overestimation for TWLV and a - 70% underestimation for TWSO at harvest (Annex 4, Table S6). Due to a larger proportion of TWSO, the NL

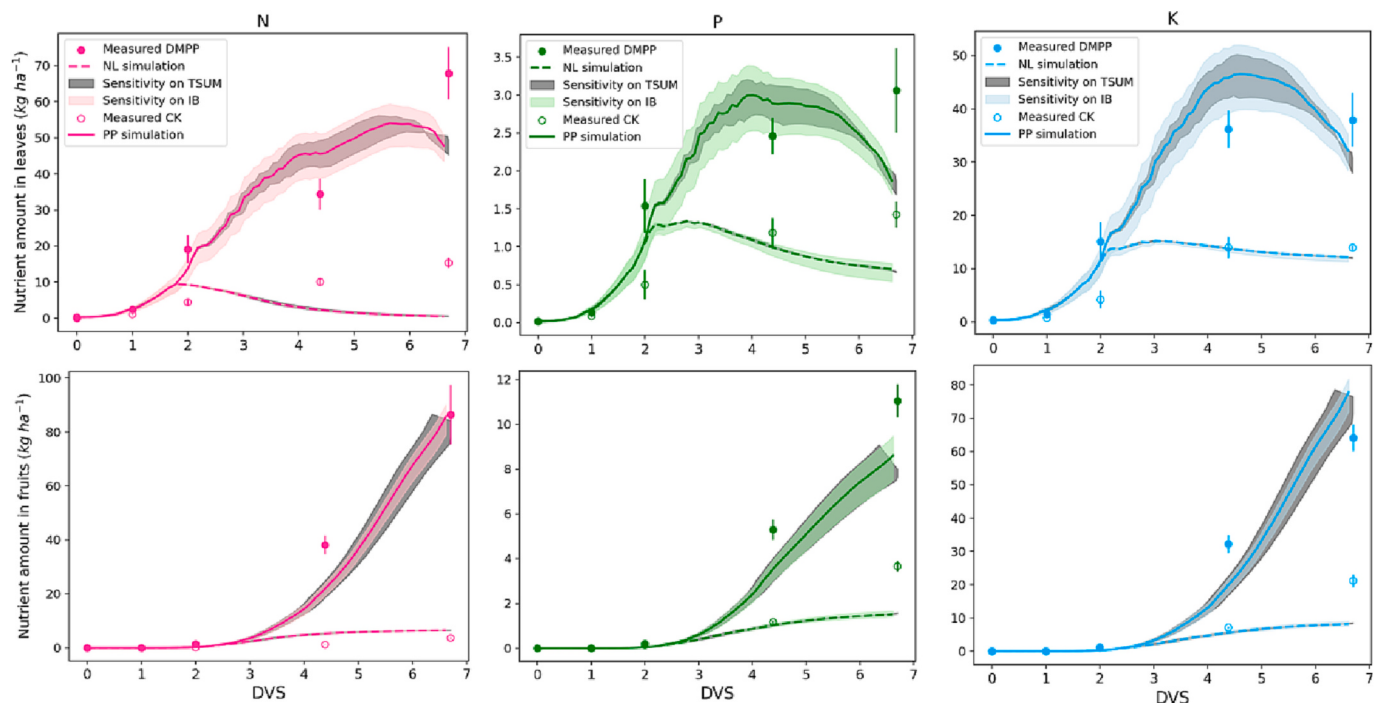


Fig. 3. Model-simulated and observed nitrogen (left) phosphorous (middle) and potassium (right) amounts in leaves (top) and fruits (bottom) for model calibration (2021), under both potential (PP, continuous lines) and nutrient-limited (NL, dashed lines) conditions. Sensitivity analysis on initial biomass ($\pm 25\%$) is shown as the light coloured area while the dark grey area represents fluctuations within ± 1 day of temperature sum from transplanting to anthesis (TSUM1).

configuration similarly underestimates TAGP (-57%) at harvest. The peak of the simulated LAI curve occurs prematurely, resulting in an overestimation at the early-fruiting stage ($+293\%$) and an underestimation at the mid-fruiting (-55%) and final harvest (-73%) stages (Fig. 2).

According to the statistical indices, R^2 values are >0.75 (good to very good model performance) for eight of twelve nutrient-uptake relevant variables. The high values of P_t (0.20–0.88) indicate insignificant differences between observed and predicted values of all nutrient-uptake variables. Most rRMSE's are >0.70 (not acceptable model performance), however, except for the PamountLV and KamountLV simulations. The NL configuration over-predicts nutrient amounts in leaves before the early-fruiting stage and predicts leaf nutrient translocation too early. Thus, the overestimated NamountLV (+136%), PamountLV (+282%), and KamountLV (+418%) at transplanting becomes underestimated NamountLV (-97%), PamountLV (-49%), and KamountLV (-13%) at harvest. The NL configuration simulates a rising fruit NPK amount, but simulated fruit P and K amounts are both underestimated by around -60% , while the NamountSO is $+72\%$ overestimated at harvest (Fig. 3, Table 4).

Overall, model performance under nutrient-limited conditions is not as good as under potential conditions. Considering the sensitivity analysis under NL conditions does not change our judgement of model performance (Figs. 2 & 3), in this case nutrient deficiency is assumed to take precedence over the influence of any other environment-related parameters on plant growth simulations.

3.4. Model validations on both potential and nutrient-limited configurations

In order to test whether WOFOST-Chili performs well in other years, we validated it using field data collected at early-fruiting, mid-fruiting, and final peak-fruiting stages in 2019 and 2020. Validated results indicate a good agreement with measured values under PP configuration in both years (Fig. 4 and Table 4; Annex 4, Fig. S4). Model simulations on leaf growth are quite satisfactory, with TWLV (rRMSE = 0.10) and

NamountLV (rRMSE = 0.16) in 2020, and TWLV (rRMSE = 0.19) and NamountLV (rRMSE = 0.17) in 2019. Model simulations on fruit growth are also acceptable, with TWSO (rRMSE = 0.23) and NamountSO (rRMSE = 0.30) in 2020, and TWSO (rRMSE = 0.46) and NamountSO (rRMSE = 0.47) in 2019. Similar to the calibrated results, a weaker model performance is found under NL configuration than PP configuration, with TWLV (rRMSE = 0.32), TWSO (rRMSE = 0.94), NamountLV (rRMSE = 0.92), and NamountSO (rRMSE = 0.85) in 2020, and TWLV (rRMSE = 0.69), TWSO (rRMSE = 0.92), NamountLV (rRMSE = 0.53), and NamountSO (rRMSE = 0.53) in 2019.

When validating the PP configuration, the model underestimates TWLV at mid-fruiting stage (-27%) in 2019 and at early-fruiting stage (-22%) in 2020. Underestimation also occurs in NamountLV at mid-fruiting stage (-23%) in 2019 and at final harvest (-17%) in 2020. The most serious underestimation occurs in fruit simulations, at -32% (2019) and -14% (2020) in TWSO and -31% (2019) and -21% (2020) in NamountSO at final harvest (Fig. 4; Annex 4, Table S6).

When validating the NL configuration, the model overestimates TWLV at early-fruiting stage ($+67\%$) in 2020, and at mid-fruiting stage ($+46\%$) and final harvest ($+116\%$) in 2019. The fruit dry weight is severely underestimated, at -71% (2019) and -76% (2020) at final harvest (Fig. 4). As for nitrogen uptake simulations, the peak of leaf N amount appears too early, resulting in the overestimation ($+2\%$ in 2019; $+69\%$ in 2020) at the early-fruiting stage and the underestimations at mid-fruiting stage (-55% in 2019; -84% in 2020) and final harvest (-89% in 2019; -97% in 2020). Fruit N amount is underestimated at the final harvest (-45%) of 2019 and the mid-fruiting stage (-35%) and final harvest (-70%) of 2020 (Fig. 4; Annex 4, Table S6).

Simulations under PP configuration are found to be sensitive to a $\pm 5\%$ adjustment of AMAXTB, EFFT, CVL, FLTB, KDIFTB, and SLATB. The most influential ranges on final total aboveground production are (-12% , $+9\%$) of FLTB (Annex 5, Fig. S8), (-12% , $+8\%$) of SLATB (Annex 5, Fig. S10) and the least influential range is (-4% , $+3\%$) of AMAXTB (Annex 5, Fig. S5). Additionally, a large change at final harvest is found by a $\pm 25\%$ IB adjustment, resulting in simulated fluctuations on TWLV (-14% , $+13\%$), TWSO (-9% , $+8\%$), NamountLV (-13% ,

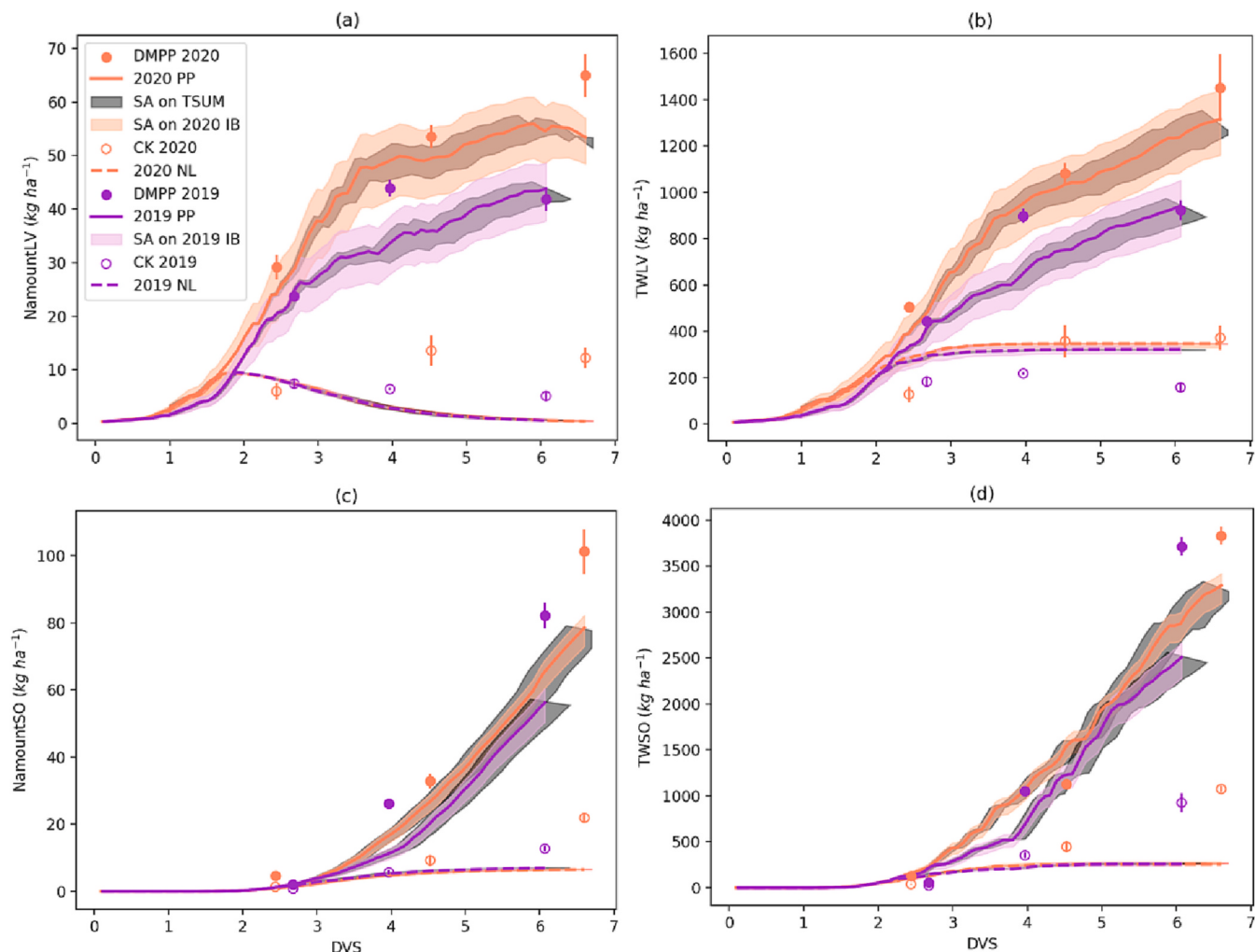


Fig. 4. Model-simulated and observed values of (a) nitrogen content in leaves (NamountLV), (b) total leaf dry weight (TWLV), (c) nitrogen content in fruits (NamountSO), and (d) total fruit dry weight (TWSO) for model validation (2019 & 2020). The purple colour represents validation results in 2019 and the orange for 2020. Error bars indicate the standard deviation of observed values. (For interpretation of the references to colour in this figure legend, the reader is referred to the web version of this article.)

+12%), and NamountSO (-11%, +7%) (Fig. 4). When adjusting the TSUM1 with the observed -12°C d (one day in advance) and $+15^{\circ}\text{C}$ d (one day postponed), the simulated NamountLV and NamountSO respond by up to (-4%, 4%) and (-2%, +2%) (Fig. 4). Similar to the results of sensitivity tests for model calibration (Fig. 2; Fig. 3), however, no obvious change under NL configuration is perceived (Fig. 4). Overall, the sensitivity analysis on model validation confirms the importance of the selected parameters on model prediction, which proves our hypothesis that model uncertainties among different years is unavoidable. This also provides the directions on where we should put efforts to decrease such variations.

4. Discussion

4.1. Model reliability on biomass-relevant simulations

Compared with other existing pepper models, WOFOST-Chili performed equally well on total aboveground production and fruit DM. The VegSyst showed very good performance on dry matter production (DMP) for one conventional pepper cultivar in 2006, with a rRMSE = 0.09 and a Wilmott index of agreement $d = 0.99$ (Giménez et al., 2013). WOFOST-Chili shows as good model performance as VegSyst, with rRMSE = 0.07 and $d = 1.00$. The simulated fruit dry matter at five different N fertilizer levels of calibrated CROPGRO-Bellpepper at maturity were all within one

standard deviation of their observed values. Similarly, WOFOST-Chili shows a smaller bias between simulated and observed values at final harvest (135 kg ha^{-1}) than the observed standard deviation ($SD \pm 231 \text{ kg ha}^{-1}$). Compared with biomass-related model variables of WOFOST-Chili, the least reliably simulated result is in the LAI simulation.

The dynamic of simulated LAI is in line with reality, increasing rapidly after anthesis, especially under fertilization, whereas the LAI peak under the no-fertilization treatment appears earlier due to premature leaf senescence (Yue et al., 2022). Unexpectedly, although the trend of simulated LAI aligns with reality, the actual values of simulated LAI were higher than what we observed. However, we believe the main reason is that we undermeasured the real LAI. We first used the YMJA portable hand-held foliar meter to measure and aggregate the LA of every leaf picked from one single plant, and then divided this by the soil area that this plant occupies, replicated the process over three plants, and took the average. In principle, this estimated LA value ignores the unevenness between plants and the shadings of branches and leaves (Fangyi et al., 2021). Moreover, we found the YMJA equipment does not fit small and irregular chili leaves. It is more suitable for flat and narrow leaves that are rich in waxy layers and not easy to shrink during measurements, such as corn leaves. In addition, our LA measurements took place in the hot summer. Chili leaves are particularly prone to water loss, wilting, shrinking, and even tearing, easily causing an underestimation of LA. As a replacement, the commonly used desktop leaf

area meter LI-3000 is recommended, because it can quickly measure a batch of leaves before water loss and wilting cause measurement errors. Furthermore, we compared our LAI data to those of 3 other chili cultivars, in their cases estimated using punch weighing method, and all of them find a larger peak LAI than our observed $\text{LAI}_{\text{pk}} = 2.00$: 'Qianla No. 10' (4.17) > 'Qianjiao No. 5' (3.37) > 'Zhongjiao No. 6' (2.61) (Yue et al., 2022). The image, grid, and paper sample weighing methods are more time-consuming, but are generally more accurate than the instrument method when measuring LA (Fangyi et al., 2021). These comparisons strongly suggest that our field observed LAI value is lower than it should be.

Our sensitivity analyses suggest that the model uncertainty of WOFOST-Chili comes from some crop initialized variables (IB) and climate-sensitive parameters (TSUM1, TSUM2, IB, AMAXTB, EFFT, CVL, FLTB, KDIFTB, and SLATB). Weaker model performance from the sensitivity analysis for the same parameters for the other 2 validation years also demonstrates that the model uncertainty of WOFOST-Chili is associated with model responses to weather inputs. Another reason for the inaccuracy of the LAI simulation may be found in the mechanism coded in the crop model. Overestimations of LAI were also found in other WOFOST studies in rice (Mukherjee et al., 2011; Roetter et al., 1998; Shekhar et al., 2008; Zhu et al., 2018), sunflower (Todorovic et al., 2009), and wheat (Castañeda-Vera et al., 2015). WOFOST calculates LAI in two stages: sink-limited exponential growth and source-limited linear growth. In the first stage, LAI is determined by the effective accumulated temperature ($^{\circ}\text{C d}$) and the maximum LAI rate per degree day (ha ha^{-1}). In the second stage, however, the LAI is determined by the daily assigned leaf weight and SLA. In fact, WOFOST keeps a complex administration on the source-limited stage of LAI, considering leaf senescence, self-shading, and the extra green area of functional stems and storage organs that absorb radiation (de Wit et al., 2020). According to Castañeda-Vera et al. (2015), the higher the complexity of the computational approach used to simulate a specific crop process, the larger its uncertainty will be. This is reasonable as complex computations normally use more parameters, and, therefore, have more complex model inner relationships. We therefore speculate that the complex mathematical logistics of source-limited LAI simulations in WOFOST may reduce the prediction accuracy to some extent. A currently hot research trend is to use LAI data derived from satellites to assist in self-correcting sensitive parameters, and then carry out model prediction. An exemplary study on soybeans has optimized parameters of field capacity, soil depth, N translocated from leaves to seed, and initial LAI based on satellite derived LAI data, and successfully improved prediction accuracy (Gasó et al., 2021). In this way, data assimilation might be a solution to overcome the limitations of process-based crop models simulating LAI, such as WOFOST-Chili.

We found the simulation accuracy of TWLV does not perform as well as TWSO and TAGP (Fig. 2). This can be explained by the fact that heavy rainfall occurred in 2021 at 40 ddt (days after transplanting) during the development phase from the early-to-mid-fruiting stages (33–60 ddt, see Annex 1, Fig. S2). Strong winds and rain at the site likely caused leaves to fall. Since we did not account for the fallen leaves in the leaf dry weight measurement, the observed leaf dry weight at the mid-fruit stage (60 ddt) was lower than the simulated value (Fig. 2). In WOFOST, TWLV is calculated by adding the dry weight of dead leaves and new leaves, and the latter is calculated by multiplying aboveground biomass with the partitioning factor to leaves (FRLV). Without counting fallen leaves, the FRLV is undercalculated, causing lower TWLV than expected. We also performed a sensitivity analysis focusing on potentially influential parameters such as TSUM1 and AMAXTB on TWLV simulation. Our results confirm the principle that the later anthesis (higher TSUM1) and higher photosynthetic efficiency (higher AMAXTB) would cause higher TWLV. To increase model accuracy, we suggest using measurements of dead leaves to calibrate death rate due to water stress, self-shading and, aging instead of using assumptions.

4.2. Model reliability on nutrient-uptake simulations

In this study we find that the dry matter simulations were more accurate than nutrient uptake simulations. A similar phenomenon is also observed in other crop model studies. For example, in the STICS-chickpea model, the RMSEs of the calibrated/validated grain yield simulations at various N application levels were N30: 0.401/0.073; N60: 0.154/0.223; and N100: 0.013/0.16, whereas the above ground production N were reported as N30: 48.86/13.24; N60: 30.81/4.03; and N100: 12.67/11.72 (Kherif et al., 2022). Apparently, STICS-chickpea also performed better for dry matter simulations than N uptake simulations. We also find that in the VegSyst-Outdoors model, dry matter production simulation of one spring spinach crop (RMSE = 0.25) outperformed the nitrogen uptake simulation (RMSE = 20.96) (Giménez et al., 2019).

In WOFOST, dynamic nutrient-uptake is calculated according to Shibu et al. (2010). Nutrient-uptake is driven by crop demand, but also depends on the available amount of nutrients that the soil can supply. Processes like mass flow and diffusion are not simulated. Instead, nutrient-uptake is simply estimated in a "book-keeping" approach. Total absorbed nutrients from both soil indigenous supply and fertilization are then partitioned among the various organs in proportion to their demands. At a certain developmental stage (often after anthesis), nutrients translocate from leaves and stems to storage organs. As chili is an indetermined crop, part of the nutrients in the leaves will still need to sustain leaf growth after anthesis and fruiting, instead of all translocating into fruits. To further improve nutrient-uptake simulations in WOFOST-Chili, new algorithms to predict the start of nutrient translocation might be needed. Unlike for nutrient dynamics, dry matter simulations use more detailed and organized dynamic processes (e.g., biomass accumulation process was set to link with temperature/DVS). We also measured more (intermediate) parameters of photosynthesis (e.g., AMAX, EFF) than nutrient processes, which further explain the better performance of WOFOST-Chili on biomass-related variables.

We attempt to explain yearly variation in nutrient uptake simulations by environmental factors. Zhou et al. (2017) concluded that variations in daily average temperature and radiation affect maize growth rate and duration of grain filling, which can lead to a change in N uptake rate. As expected, the lower radiation and more rainy days in year 2019 were found to cause lower simulated values of nutrients amount in chili than in 2020 and 2021. However, WOFOST-Chili does not account for the possibility that the lower part of chili canopy might better absorb diffuse light to cope with such adverse conditions. Therefore, a larger gap between the simulated and observed nutrient amounts was found in 2019. Another objective reason is that parameters that are sensitive to temperature and radiation (e.g., SLA) could vary between different years, but were only calibrated with the one-time measurement data from 2021.

4.3. Model reliability on nutrient-limited configuration

In this study, similar to other model studies, we found better simulation results under PP configuration than under NL configuration. One AquaCrop-maize study showed that the lowest uncertainty of estimated yield was under the minimal water and N stresses (Guo et al., 2020). Another maize model study of HYDRUS-2D recognized different levels of prediction accuracy of N uptake when under different N fertilizations (Ranjbar et al., 2022). One study of STICS-chickpea also found that N uptake by above ground biomass was simulated worse under low N-application (30 kg N ha^{-1}) than under moderate (60 kg N ha^{-1}) and high (100 kg N ha^{-1}) N rates (Kherif et al., 2022).

It should not come as a surprise that the potential growth configuration performs better since it is always the starting point for building a new crop model. WOFOST brings a new concept of "nutrient stress" when developing the NL configuration. It assumes that nutrient stress effects can be modelled by multiplying nutrient-related stress coefficients on the assimilation rate, the dry matter partitioning to leaves,

and the leaf extension rate. In *WOFOST-Chili*, the nutrient stress coefficients (e.g., NLAI_NPK, NLUE_NPK) are represented by single values. Inspired by one dynamic LAI model of chili under different N levels established by Yue et al. (2022), intermediate measurable parameters (e.g., increase and decrease rate of LAI) are linked with different nutrient supply levels. If we could describe the nutrient stress coefficients as a function of dynamic changes of DVS, and then link the DVS with fertilizer levels or other potential influential environmental factors such as temperature, we may decrease model uncertainty under NL configuration.

4.4. Future prospects on *WOFOST-chili*

Our study shows that it is possible to use *WOFOST* to simulate chili pepper growth and development without changing much from the generic model structure. We provide solutions by adapting user-defined developmental stages to mimic the growth from transplanting to fruiting, and subsequently to ripeness. This newly developed method could be used as a reference to expand the application of crop models originally designed for cereals to vegetables and other non-cereal crops, which will help to fill blank research areas of those process-based crop models.

Being able to track nutrient-uptake responses with and without fertilizer applications, *WOFOST-Chili* would assist in calculating potential leaching from soil to water systems, which is valuable to guide sustainable fertilizer strategies. The current model only simulates crop response to two extreme statuses of fertilizer applications (optimal and nutrient deficiency conditions), while simulations with more fertilizer gradients could be further addressed in the future. To better model fertilizer response to dry yield and nutrient uptake, we also call for a refined dynamic nutrient flow description in the soil module to evaluate the effect of expanded fertilizer strategies, such as using new fertilizer products (e.g., organic fertilizer, denitrification products, and slow-control-release fertilizers).

Due to the high laboratory costs of the NPK analyses, soil testing and formula fertilization technology may not be realistic for many regions. Fortunately, with more cheaper instruments for immediate crop N status measurement available, such as the SPAD® (Minolta), the Hydro N-Tester® (Yara), the N-sensor® (Yara) and the ®GPN (Grande Paroisse) (Naud et al., 2008), testing nutrient-uptake simulations on a larger scale becomes feasible. This will accelerate the model improvement progress.

Since the original *WOFOST-generic* model was designed for cereal crops, *WOFOST-Chili* has some limitations. The nutrient translocation process should be further improved to match the simultaneous growth of leaves and fruits after anthesis. Also, it is essential to test the model for other locations with other climatic conditions and crop planting times. The evaluation of the model's transferability suggested that further research should concentrate on the initial stages of crop development, and especially on climate-sensitive parameters when expanding *WOFOST-Chili* to different growing years.

More broadly, with climate change potentially negatively affecting chili production, *WOFOST-Chili* could be valuable for providing adaptation options. For example, it could be used to guide the adjustment of sowing and harvesting dates, or even guiding the reallocation of suitable growing areas. It could be also used to evaluate alternative fertilizer and irrigation strategies, or guide the development of new chili cultivars. Based on model outcomes, *WOFOST-Chili* may help guarantee chili production capacity in a resource-efficient way under climate change, contributing to Sustainable Development Goals of zero hunger (SDG2) and climate action (SDG13).

5. Conclusion

We adapted a new version *WOFOST-Chili* from the generic *WOFOST* model to simulate the development, dry matter production, and nutrient uptake of chili peppers. This newly developed *WOFOST-Chili* was tested

using original field trial data over three consecutive years. Additionally, we conducted a systematic sensitivity analysis and increased the robustness of *WOFOST-Chili*. Our results indicated that *WOFOST-Chili* performs reliably in simulating potential growth over three growing years, as evidenced by the rRMSE values of 0.10–0.23 for the dry weight of leaves, 0.06–0.46 for fruits, 0.07–0.30 for total aboveground biomass. *WOFOST-Chili* also accurately predicted the N/P/K amounts within leaves (rRMSE = 0.16–0.46) and fruits (rRMSE = 0.29–0.47). Moreover, *WOFOST-Chili* was found to be able to distinguish simulations under potential and nutrient limited conditions. To further improve nutrient-uptake simulations in *WOFOST-Chili*, new algorithms to predict the start of nutrient translocation might be needed. To conclude, our study provides insight on expanding the application of crop models originally designed for cereals to non-Gramineae vegetables without substantial changes to the generic model structure. Our study can support fertilizer-efficient management in open-field vegetable production under climate change to achieve SDG2 (food security) and SDG13 (climate action).

CRediT authorship contribution statement

Ruoling Tang: Investigation, Methodology, Software, Writing – original draft. **Iwan Supit:** Supervision, Software, Writing – review & editing. **Ronald Hutjes:** Supervision, Writing – review & editing, Conceptualization. **Fen Zhang:** Investigation. **Xiaozhong Wang:** Writing – review & editing. **Xuanjing Chen:** Supervision, Writing – review & editing. **Fusuo Zhang:** Funding acquisition. **Xinping Chen:** Supervision, Resources, Conceptualization.

Declaration of Competing Interest

The authors declare that they have no known competing financial interests or personal relationships that could have appeared to influence the work reported in this paper.

Data availability

Data will be made available on request.

Acknowledgments

This work was supported by the National Natural Science Foundation of China (NSFC, grant no. U20A2047 and 42107056). We also thank Bryan Marinelli (Wageningen University) for careful language editing assistance, which greatly improved the clarity and readability of the manuscript.

Appendix A. Supplementary data

Supplementary data to this article can be found online at <https://doi.org/10.1016/j.agsy.2023.103688>.

References

- Baena, N., Belović, M., Ilic, N., Moreno, D.A., García-Viguera, C., 2019. Industrial use of pepper (*Capsicum annuum* L.) derived products: technological benefits and biological advantages. *Food Chem.* 274, 872–885. <https://doi.org/10.1016/j.foodchem.2018.09.047>.
- Boogaard, H., De Wit, A., te Röller, J., Van Diepen, C., Rötter, R., Cabrera, J., van Laar, H., 2014. WOFOST control Centre 2.1 and WOFOST 7.1. 7. User's guide for the WOFOST control Centre 2.1 and WOFOST 7.1.7 crop growth simulation model. Alterra Wageningen University & Research Centre, Wageningen, p. 133. <http://www.wur.nl/web/file?uid=5e0873c3-8c07-4ddf-85a3-dd98bdb38781&owner=b875561e-c6d9-442d-b599-58e9d13cb80d>.
- Boote, K.J., Hoogenboom, G., Jones, J.W., Ingram, K.T., 2008. Modeling Nitrogen Fixation and its Relationship to Nitrogen Uptake in the CROPGRO Model, Quantifying and Understanding Plant Nitrogen Uptake for Systems Modeling. CRC Press, pp. 13–46. <https://doi.org/10.1201/9781420052978>.
- Boote, K.J., Jones, J.W., Hoogenboom, G., 2018. Simulation of Crop Growth: CROPGRO Model, Agricultural Systems Modelling and Simulation. CRC Press, pp. 651–692. <https://doi.org/10.1201/9781482269765>.

- Bosi, C., Sentelhas, P.C., Pezzopane, J.R.M., Santos, P.M., 2020. CROPGRO-perennial forage model parameterization for simulating Piatã palisade grass growth in monoculture and in a silvopastoral system. *Agric. Syst.* 177, 102724 <https://doi.org/10.1016/j.agrsy.2019.102724>.
- Bremner, J.M., 1996. Nitrogen-total. Methods of soil analysis: part 3. Chemical methods 5, 1085–1121. <https://doi.org/10.2136/sssabookser5.3.c37>.
- Cammarano, D., Jamshidi, S., Hoogenboom, G., Ruane, A.C., Niyogi, D., Ronga, D., 2022. Processing tomato production is expected to decrease by 2050 due to the projected increase in temperature. *Nature Food* 3, 437–444. <https://doi.org/10.1038/s43016-022-00560-5>.
- Castañeda-Vera, A., Leffelaar, P.A., Álvaro-Fuentes, J., Cantero-Martínez, C., Minguez, M., 2015. Selecting crop models for decision making in wheat insurance. *Eur. J. Agron.* 68, 97–116. <https://doi.org/10.1016/j.eja.2015.04.008>.
- de Wit, A.J.W., Boogaard, H.L., Supit, I., van den Berg, M., 2020. System description of the WOFOST 7.2, cropping systems model. (rev. 1.1 ed.). Wageningen Environmental Research. <https://edepot.wur.nl/522204>.
- Di Paola, A., Valentini, R., Santini, M., 2016. An overview of available crop growth and yield models for studies and assessments in agriculture. *J. Sci. Food Agric.* 96, 709–714. <https://doi.org/10.1002/jsfa.7359>.
- Diao, M., Dai, J., Luo, W., Yuan, C., Bu, C., Xian, K., Zhang, S., Xu, R., 2009. Model for simulation of growth and yield of greenhouse sweet pepper. *Transactions of the Chinese Society of Agricultural Engineering* 25, 241–246. <https://doi.org/10.3969/j.issn.1002-6819.2009.10.044>.
- Deltra, J., Muñoz, P., 2010. Simulation of nitrogen leaching from a fertigated crop rotation in a Mediterranean climate using the EU-Rotate_N and Hydrus-2D models. *Agric. Water Manag.* 97, 277–285. <https://doi.org/10.1016/j.agwat.2009.09.019>.
- Fangyi, L., Huang, H., Chunyun, G., 2021. Review on measurement of crop leaf area. *Journal of Hunan Agricultural University(Natural Sciences)* 47, 274–282. <https://doi.org/10.13331/j.cnki.jhau.2021.03.005>.
- FAOSTAT, 2020. Crops and Livestock Products.
- Gallardo, M., Fernández, M.D., Giménez, C., Padilla, F.M., Thompson, R.B., 2016. Revised VegSyst model to calculate dry matter production, critical N uptake and ETc of several vegetable species grown in Mediterranean greenhouses. *Agric. Syst.* 146, 30–43. <https://doi.org/10.1016/j.agrsy.2016.03.014>.
- Gaso, D.V., de Wit, A., Berger, A.G., Kooistra, L., 2021. Predicting within-field soybean yield variability by coupling Sentinel-2 leaf area index with a crop growth model. *Agric. For. Meteorol.* 308, 108553 <https://doi.org/10.1016/j.agrmet.2021.108553>.
- Gijzen, H., 1994. Development of a simulation model for transpiration and water uptake and an integral growth model. AB-DLO Report 18, 90.
- Giménez, C., Gallardo, M., Martínez-Gaitán, C., Stöckle, C., Thompson, R., Granados, M., 2013. VegSyst, a simulation model of daily crop growth, nitrogen uptake and evapotranspiration for pepper crops for use in an on-farm decision support system. *Irrig. Sci.* 31, 465–477. <https://doi.org/10.1007/s00271-011-0312-2>.
- Giménez, C., Thompson, R., Prieto, M., Suárez-Rey, E., Padilla, F., Gallardo, M., 2019. Adaptation of the VegSyst model to outdoor conditions for leafy vegetables and processing tomato. *Agric. Syst.* 171, 51–64.
- Guo, D., Zhao, R., Xing, X., Ma, X., 2020. Global sensitivity and uncertainty analysis of the AquaCrop model for maize under different irrigation and fertilizer management conditions. *Arch. Agron. Soil Sci.* 66, 1115–1133. <https://doi.org/10.1080/03650340.2019.1657845>.
- Kadigi, I.L., Richardson, J.W., Mutabazi, K.D., Philip, D., Mourice, S.K., Mbungu, W., Buzimana, J.-C., Sieber, S., 2020. The effect of nitrogen-fertilizer and optimal plant population on the profitability of maize plots in the Wami River sub-basin, Tanzania: a bio-economic simulation approach. *Agric. Syst.* 185, 102948 <https://doi.org/10.1016/j.agrsy.2020.102948>.
- Kaur, M., Verma, B.R., Zhou, L., Lak, H.M., Kaur, S., Sammour, Y.M., Kapadia, S.R., Grimm, R.A., Griffin, B.P., Xu, B., 2022. Association of pepper intake with all-cause and specific cause mortality - a systematic review and meta-analysis. *Am J Prev Cardiol* 9, 100301. <https://doi.org/10.1016/j.apjc.2021.100301>.
- Khaitov, B., Umurzakov, M., Cho, K.-M., Lee, Y.-J., Park, K.W., Sung, J., 2019. Importance and production of chilli pepper; heat tolerance and efficient nutrient use under climate change conditions. *Korean Journal of Agricultural Science* 46, 769–779. <https://doi.org/10.7744/kjoas.20190059>.
- Kherif, O., Seghouani, M., Justes, E., Plaza-Bonilla, D., Bouhenache, A., Zemmouri, B., Dokukin, P., Latati, M., 2022. The first calibration and evaluation of the STICS soil-crop model on chickpea-based intercropping system under Mediterranean conditions. *Eur. J. Agron.* 133, 126449 <https://doi.org/10.1016/j.eja.2021.126449>.
- Liu, H., Yang, H., Zheng, J., Jia, D., Wang, J., Li, Y., Huang, G., 2012. Irrigation scheduling strategies based on soil matric potential on yield and fruit quality of mulched-drip irrigated chili pepper in Northwest China. *Agric. Water Manag.* 115, 232–241. <https://doi.org/10.1016/j.agwat.2012.09.009>.
- Liu, Z., Ying, H., Chen, M., Bai, J., Xue, Y., Yin, Y., Batchelor, W.D., Yang, Y., Bai, Z., Du, M., 2021. Optimization of China's maize and soy production can ensure feed sufficiency at lower nitrogen and carbon footprints. *Nature Food* 2, 426–433. <https://doi.org/10.1038/s43016-021-00300-1>.
- Lu, C., Tian, H., 2017. Global nitrogen and phosphorus fertilizer use for agriculture production in the past half century: shifted hot spots and nutrient imbalance. *Earth System Science Data* 9, 181–192. <https://doi.org/10.5194/essd-9-181-2017>.
- Marcelis, L., 1994. A simulation model for dry matter partitioning in cucumber. *Ann. Bot.* 74, 43–52. <https://doi.org/10.1006/anbo.1994.1092>.
- Marcelis, L., De Groot, C., Del Amor, F., Elings, A., Heinen, M., De Visser, P., 2003. Crop Nutrient Requirements and Management in Protected Cultivation.
- Marcelis, L., Brajeul, E., Elings, A., Garate, A., Heuvelink, E., De Visser, P., 2004. Modelling nutrient uptake of sweet pepper, international conference on sustainable greenhouse systems. *Greensys* 691, 285–292. <https://doi.org/10.17660/ActaHortic.2005.691.33>.
- Meier, U., 1997. Growth stages of mono-and dicotyledonous plants. Blackwell Wissenschafts-Verlag. <https://agris.fao.org/agris-search/search.do?recordID=US201300311612>.
- Mendez, M.M., 2000. Development and Use of a Pepper Growth Simulation Model. University of Puerto Rico, Mayaguez (Puerto Rico).
- Moriasi, D.N., Arnold, J.G., Van Liew, M.W., Bingner, R.L., Harmel, R.D., Veith, T.L., 2007. Model evaluation guidelines for systematic quantification of accuracy in watershed simulations. *Trans. ASABE* 50, 885–900. <https://doi.org/10.13031/2013.23153>.
- Mukherjee, J., Singh, L., Singh, G., Bal, S., Singh, H., Kaur, P., 2011. Comparative evaluation of WOFOST and ORYZA2000 models in simulating growth and development of rice (*ORYZA sativa* L.) in Punjab. *Journal of Agrometeorology* 13, 86–91. <https://doi.org/10.54386/jam.v13i2.1347>.
- Naud, C., Makowski, D., Jeuffroy, M.-H., 2008. Is it useful to combine measurements taken during the growing season with a dynamic model to predict the nitrogen status of winter wheat? *Eur. J. Agron.* 28, 291–300. <https://doi.org/10.1016/j.eja.2007.08.005>.
- Øvsthus, I., Thorup-Kristensen, K., Seljåsen, R., Riley, H., Dörsch, P., Breland, T.A., 2021. Calibration of the EU-Rotate_N model with measured C and N mineralization from potential fertilizers and evaluation of its prediction of crop and soil data from a vegetable field trial. *Eur. J. Agron.* 129, 126336. <https://doi.org/10.1016/j.eja.2021.126336>.
- Prioul, J., Chartier, P., 1977. Partitioning of transfer and carboxylation components of intracellular resistance to photosynthetic CO₂ fixation: a critical analysis of the methods used. *Ann. Bot.* 41, 789–800. <https://doi.org/10.1093/oxfordjournals.aob.a085354>.
- Producepay, 2021. Chili Pepper Production Zones in Mexico. <https://producepay.com/chili-pepper-production-zones-in-mexico>.
- Ranjbar, A., Rahimikhoob, A., Ebrahimiyan, H., Varavipour, M., 2022. Simulation of nitrogen uptake and dry matter for estimation of nitrogen nutrition index during the maize growth period. *J. Plant Nutr.* 45, 920–936. <https://doi.org/10.1080/01904167.2021.1994603>.
- Reddy, A., Tiwari, K., 2018. Assessment of CROPGRO-Bellpepper model under different nitrogen levels through fertigation. *International Journal of Agricultural Engineering* 11, 101–107. <https://doi.org/10.15740/IJAE/11.1/101-107>.
- Roetter, R., Hoanh, C.T., Teng, P.S., 1998. A systems approach to analyzing land use options for sustainable rural development in South and Southeast Asia. <https://doi.org/10.22004/ag.econ.28750>.
- Salo, T.J., Palosuo, T., Kersebaum, K.C., Nendel, C., Angulo, C., Ewert, F., Bindl, M., Calanca, P., Klein, T., Moriondo, M., 2016. Comparing the performance of 11 crop simulation models in predicting yield response to nitrogen fertilization. *J. Agric. Sci.* 154, 1218–1240. <https://doi.org/10.1017/S0021859615001124>.
- Saqib, M., Anjum, M.A., 2021. Applications of decision support system: a case study of solanaceous vegetables. *Phyton* 90, 331. <https://doi.org/10.32604/phyton.2021.011685>.
- Shekhar, C., Singh, D., Singh, R., Rao, V., 2008. Prediction of wheat growth and yield using WOFOST model. *Journal of Agrometeorology* 400 (Special issue-Part 2), 402. <https://www.agrometassociation.org/journal-view/journal-of-agrometeorology>.
- Shibu, M.E., Leffelaar, P.A., van Keulen, H., Aggarwal, P.K., 2010. LINTUL3, a simulation model for nitrogen-limited situations: application to rice. *Eur. J. Agron.* 32, 255–271. <https://doi.org/10.1016/j.eja.2010.01.003>.
- Stan, T., Munteanu, N., Teliban, G.-C., Cojocaru, A., Stoleru, V., 2021. Fertilization management improves the yield and Capsaicinoid content of chili peppers. *Agriculture* 11, 181. <https://doi.org/10.3390/agriculture11020181>.
- Tahir, N., Li, J., Ma, Y., Ullah, A., Zhu, P., Peng, C., Hussain, B., Danish, S., 2021. 20 years nitrogen dynamics study by using APSIM nitrogen model simulation for sustainable management in Jilin China. *Sci. Rep.* 11, 1–21. <https://doi.org/10.1038/s41598-021-96386-5>.
- Tei, F., De Neve, S., de Haan, J., Kristensen, H.L., 2020. Nitrogen management of vegetable crops. *Agric. Water Manag.* 240, 106316 <https://doi.org/10.1016/j.agwat.2020.106316>.
- Timsina, J., Dutta, S., Devkota, K.P., Chakraborty, S., Neupane, R.K., Bisht, S., Amgain, L.P., Singh, V.K., Islam, S., Majumdar, K., 2021. Improved nutrient management in cereals using nutrient expert and machine learning tools: productivity, profitability and nutrient use efficiency. *Agric. Syst.* 192, 103181 <https://doi.org/10.1016/j.agrsy.2021.103181>.
- Todorovic, M., Albrizio, R., Zivotic, L., Saab, M.T.A., Stöckle, C., Steduto, P., 2009. Assessment of AquaCrop, CropSyst, and WOFOST models in the simulation of sunflower growth under different water regimes. *Agron. J.* 101, 509–521. <https://doi.org/10.2134/agronj2008.0166s>.
- Wang, X., Liu, B., Wu, G., Sun, Y., Guo, X., Jin, Z., Xu, W., Zhao, Y., Zhang, F., Zou, C., Chen, X., 2018. Environmental costs and mitigation potential in plastic-greenhouse pepper production system in China: a life cycle assessment. *Agric. Syst.* 167, 186–194. <https://doi.org/10.1016/j.agrsy.2018.09.013>.
- Yue, Y., Li, R., Feng, E., Li, L., Peng, S., Sun, C., 2022. Dynamic simulation of leaf area index of pepper under different nitrogen levels. *Journal of China Agricultural University* 27, 157–168. <https://doi.org/10.3390/agronomy8090172>.
- Zerulla, W., Barth, T., Dressel, J., Erhardt, K., Horchler von Locquenghien, K., Pasda, G., Rädle, M., Wissemeyer, A., 2001. 3, 4-Dimethylpyrazole phosphate (DMPP)—a new

- nitrification inhibitor for agriculture and horticulture. *Biol. Fertil. Soils* 34, 79–84. <https://doi.org/10.1007/s003740100380>.
- Zhou, B., Yue, Y., Sun, X., Ding, Z., Ma, W., Zhao, M., 2017. Maize kernel weight responses to sowing date-associated variation in weather conditions. *The Crop Journal* 5, 43–51. <https://doi.org/10.1016/j.cj.2016.07.002>.
- Zhu, J., Zeng, W., Ma, T., Lei, G., Zha, Y., Fang, Y., Wu, J., Huang, J., 2018. Testing and improving the WOFOST model for sunflower simulation on saline soils of Inner Mongolia, China. *Agronomy* 8, 172. <https://doi.org/10.3390/agronomy8090172>.